Boundary Searching Snakes for Segmenting Noisy Images

Jiankang Wang
Department of Computing Science
University of Alberta
Edmonton, AB, Canada T6G 2H1
e-mail: jiankang@cs.ualberta.ca

Xiaobo Li
Department of Computing Science
University of Alberta
Edmonton, AB, Canada T6G 2H1
e-mail: li@cs.ualberta.ca

Andrew Bradley
Canon Information Systems Research Australia (CISRA)
1 Thomas Holt Drive
North Ryde, Australia NSW 2113
e-mail: bradley@research.canon.com.au

Abstract

In this paper we propose a snake model that is suitable for the segmentation of noisy images. The proposed snake model, which we call a *boundary searching snake*, is created by incorporating a searching strategy into some common snake techniques. The searching strategy is achieved by systematically changing the artificial *normal force* applied to the snake. The force is chosen to be initially large and outgoing, but is flipped in direction and reduced in magnitude after reaching equilibrium. The process stops when the normal force is small compared to other snake forces, i.e., when a global minimum is found. The searching strategy makes it possible for a part of the snake to backtrack to areas previously visited and look for weaker features, a property that is crucial in the segmentation of noisy images. We demonstrate the technique using Ivins and Porrill's active region model and further suggest a number of other improvements to this model: (1) an adaptive feature is added to the model so that it can cope with images with slowly changing intensity values; (2) the internal energy is reformulated to get rid of the shrinking force in the original formulation; and (3) the re-parameterization procedure is improved to avoid impairing the stretch-resisting force. The new method is tested on both real and synthetic images and results show some promise.

Keywords: **noisy image segmentation, snakes, boundary searching snakes**

1 Introduction

The active contour models (ACMs), or snakes, were first proposed by Kass *et al.* [5] as a regularization approach to the ill-posed edge detection problem. A snake is a smooth spline under the influence of image forces and internal constraint forces. The internal spline forces serve to impose a smoothness constraint on the detected edges. The image forces push the snake towards salient image features like lines, edges, and subjective contours.

The snake model is an analogy of mechanical systems; influencing forces can be represented by equivalent potential and kinetic energy. Snake movement is governed by minimization of the total energy. Representing the position of a snake parametrically by $\mathbf{v}(s) = \mathbf{v}(x(s), y(s))$ where s is the spatial index, we can write its energy functional as[1]

$$E_{snake} = \oint (E_{int}(\mathbf{v}) + E_{ext}(\mathbf{v}))ds \qquad (1)$$

where E_{int} represents the internal energy of the spline due to bending and stretching and E_{ext} gives rise to the external constraint and image forces. Various methods have been used to minimize the energy including variational calculus [6], dynamic programming [8], and greedy heuristic searches [9].

There are several problems with the original snake formulation including: (1) a user provided initialization, which should be very close to the desired object boundary, is required; and (2) a snake could be easily trapped by local minima. A number of

[1] We only discuss closed snakes in this paper.

people have proposed solutions to these problems. Berger [1] proposed a method called *snake growing* to try to eliminate the snake initialization problem. However, his method loses the desirable global property of the snake model because in his model, snakes start from edges selected from an edge map and grow at the two ends. It has no global model and thus can only fill small gaps. To cope with the initialization problem, Cohen and Cohen [2] proposed a *balloon* model which uses an inflating force to make the contour expand until it meets an object boundary. However, as pointed out by Xu *et al.* [10] a snake tends to shrink due to its internal forces and even worse, the internal forces are not homogeneous along the boundary, being large at points with high curvature. This makes it difficult to choose a constant inflating force for the balloon model. Gunn and Nixon [3] presented a dual snake scheme with one snake starting from outside the object boundary and one from inside. The process stops when the two snakes meet each other. Although this scheme greatly reduces the sensitivity of a snake to its initial position, it is still possible to be trapped in local minima. Moreover, in places where there are not any strong features, the final position of the snakes is undetermined, depending on how fast the two snakes move.

In this paper, we propose a method called the boundary searching snake to solve the above two problems. Our aim is to develop a method that could be used to segment noisy images, such as ultrasound and infrared images. Our research was also inspired by human behavior: when we try to localize an object boundary, we usually seek information from its neighboring areas. This process is to search for more evidence either to reinforce the decision we have made or to correct it.

The remainder of this paper is organized as follows: Section 2 talks about the searching strategy which is the main contribution of this paper. Section 3 presents an implementation of the boundary searching snake based on the active region models proposed by Ivins and Porrill [4]. The active region models are modified to integrate region and edge information and are further improved in several other ways. Experimental results for both synthetic and real images are presented in Section 4. Section 5 discusses problems with our method and outlines future work.

2 The Boundary Searching Snake

One of the reasons that a snake is sensitive to its initialization is because of the existence of multiple local minima, especially in noisy images. The balloon model partially solves this problem by pushing the snake out of local minima using an artificial inflating force. However, this poses a problem in that an appropriate inflating force is not easy to choose. If the balloon force is chosen to be too large, the snake will skip over strong features. On the other hand, if the inflating force is small in comparison with other forces, it does not have the desired effect. A compromise is difficult to achieve, especially in the case of noisy images, bacause there are both weak and strong features that must be extracted from the same image.

The boundary searching snake model is proposed to solve the above problem. Our strategy is to change the artificial inflating force systematically. Just like the balloon model, we start with a snake with a large outgoing normal force, *i.e.*, an *inflating* force. The force is chosen to be large enough to skip weak edges yet small enough to be offset by strong edges. This could be achieved by an analysis of the edge magnitude histogram or by experience. When it comes to equilibrium, the normal force is changed to the opposite direction and its magnitude is reduced *e.g.*, to 80%. This is to search for weaker features which may have been skipped in the first round. The whole procedure is repeated until the normal force is small enough to be ignored. Hopefully, by then we will have found a solution which is the global minimum.

An illustration is shown in Fig. 1. The snake starts from contour A and the object boundary of interest is B. There are some big gaps along the boundary as is the case for edges derived from real life noisy images. For the same reason, the intensity around the gaps is not enough to make the snake stop. Thus a possible result is shown in the figure as boundary C, which is over-inflated if taken as a balloon. The major force that makes it stop at point C is the internal stretch-resisting force from other parts of the boundary. Once it has reached the first equilibrium, the normal force is flipped in direction and reduced in magnitude. This makes the snake backtrack to places previously visited and look for weaker features.

This snake model has the good property of the balloon model and yet eliminates the difficulty of choosing a weight for the normal force. In ultrasound and infrared images, features may be weak

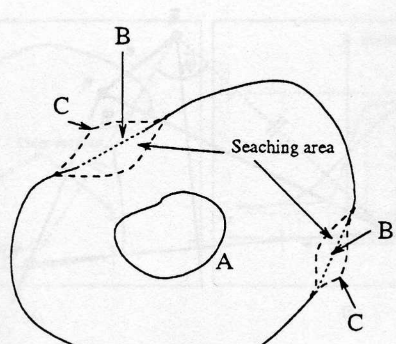

Figure 1: An illustration of the boundary searching snake.

due to low contrast and noise corruption. The snake model we have proposed is able to use weak information and this property is crucial in segmenting noisy images. Moreover, our snake model is less sensitive to its initialization since it is not trapped in local minima as easily as other snake models. This property is important to automatic segmentation since this way there is no need to have an operator to specify an initialization or another program to provide one.

Since the snake is regularized by its internal energy, a piece of boundary will not "pop out" when it is stopped by the internal forces from parts that are already stopped by strong edges or region information (boundary C of Fig. 1). Thus, the searching space should be restricted, and the extra computation cost should not be significant.

3 Implementation Based on Active Region Models

The searching strategy is a general idea and could be applied to any variants of Kass' snake model [5]. In this paper, we use the active region models (ARMs) proposed by Ivins and Porrill [4] since both region and edge information could be exploited by this model. This is important in processing noisy images since in these images, no single feature is reliable. Using multiple features can increase the reliability of the segmentation process.

The fast greedy heuristic search algorithm [9] is used for energy minimization. In the implementation, a discrete version of the snake model, which consists of a set of nodes called snaxels, is used. For each snaxel, its eight neighbors are checked and the position which has the lowest energy is chosen as the destination. The iteration stops when no snaxel can be further moved to lower the total energy. The method used to compute the energies for each snaxel is discussed below. We improved the active region models in several ways: (1) an adaptive feature is added so that the snakes can cope with images with slowly changing intensities; (2) the internal energy is re-formulated to get rid of the shrinking effect of the original internal energy formulation; and (3) the re-parameterization procedure [4] is improved to keep the internal stretch-resisting force.

3.1 An Adaptive Feature

Active region models could be thought of as pressurized region-growers. An ARM starts from a seed region and expands until its elements meet pixels that exceed user-defined limits relative to the seed region. A new energy term called *region* energy, which generates a pressure force from the pixels inside the region enclosed by the model to make the ARM expand or shrink, is used in the model. The energy composition is:

$$\begin{aligned} E_{snake} = \ & \oint E_{int}(\mathbf{v})ds - \rho(s) \iint_R G(I(x,y))dxdy \\ & -\kappa(s) \oint P(I(x,y))ds \end{aligned} \quad (2)$$

where G is a functional that measures the *goodness* of pixels within the region R of an image $I(x,y)$ enclosed by an ARM $\mathbf{v}(s)$, and $P(I(x,y))$ is a potential field derived from the image intensity.

The functional G is chosen as

$$G(I(x,y)) = 1 - \frac{Z}{k} \quad (3)$$

$$Z = \left| \frac{A(I(x,y)) - \mu}{\sigma} \right| \quad (4)$$

where k is a constant which is typically 2 or 3. The intensity mean, μ, and standard deviation, σ, are computed from the seed region. $A(I(x,y))$ is the average intensity value on the boundary between the current snaxel and its two neighbors, *i.e.* its successor and predecessor along the boundary. To make the snake adaptive to intensity changes, we propose to have each snaxel associated with a μ. Whenever a snaxel is moved, its mean, μ, is updated as follows:

$$\mu = \mu - \frac{1}{\ell}(\mu - \mu_{\mathbf{v}}) \cdot \cos(\phi) \quad (5)$$

where ℓ is a constant with typical value 5 or 6, $\mu_{\mathbf{v}}$ is the average intensity value around $\mathbf{v}$, and ϕ is the angle between the normal direction and the moving direction[2]. To make it more reliable, some conditions could be checked before the mean value is

[2]The moving direction is from the current position of a snaxel to its next position.

updated: (1) that the region force is larger than a pre-defined threshold; and (2) that the moving angle is less than a pre-defined value. These two conditions would ensure that the mean value is only changed by slowly changing intensity values. Moreover, both the original and updated mean could be used in calculating the region energy. This way by setting appropriate weights for the two means, we can control how adaptive we want the snake be. In the present implementation, standard deviation remains unchanged.

As mentioned before, a discrete snake model is used. For each snaxel, each of its eight neighbors could be possible destination. The region energy is calculated using the following formula [4]:

$$\delta \mathbf{E}_{region} \approx -\frac{\rho}{2} \oint G(I(\mathbf{v})) \left(\frac{\partial \mathbf{v}}{\partial s}\right)^{\perp} \cdot \delta \mathbf{v} ds \quad (6)$$

where $(\frac{\partial \mathbf{v}}{\partial s})^{\perp}$ is the normal unit vector. $\delta \mathbf{v}$ is a small change to the snake and $\delta \mathbf{E}_{region}$ is the corresponding energy change.

3.2 Internal Energy Reformulation

As discussed in Section 1, the shrinking force from the internal energy makes it difficult to choose a normal force so that it has the same effect along the whole boundary. To solve this problem, we adopt the internal energy formulation proposed by Gunn and Nixon [3] in our model. This formulation does not have a shrinking effect. Moreover, it is proven to be invariant to scale, translation, and rotation [3].

For simplicity of computation, the contour, which consists of N snaxels, is described in an anti-clockwise manner. The first condition is to make the snaxels stay equi-distant:

$$|\mathbf{v}_{i-1} - \mathbf{v}_i| = |\mathbf{v}_{i+1} - \mathbf{v}_i| \quad (7)$$

and the energy formulation for this part is:

$$E_{int(I)}(\mathbf{v}_i) = \left|1 - \frac{\mathbf{d}_{i-1}}{h}\right| \quad (8)$$

where $\mathbf{d}_i$ stands for distance between snaxel $\mathbf{v}_i$ and $\mathbf{v}_{i+1}$, and h is the average distance between snaxels. The second condition is to make each snaxel move to a place that is predicted by its two neighbors. As shown in Fig. 2, the predicted position for $\mathbf{v}_i$ is $\tilde{\mathbf{v}}_i$ which, along with $\mathbf{v}_{i+1}$ and $\mathbf{v}_{i-1}$, constructs an isosceles triangle with $\tilde{\psi}_i$ equal to $\frac{1}{N}\sum_{i=0}^{N-1} \psi_i$. We write:

$$\begin{aligned} \mathbf{e}_i &= \tilde{\mathbf{v}}_i - \mathbf{v}_i = \tfrac{1}{2}(\mathbf{v}_{i-1} + \mathbf{v}_{i+1}) - \\ &\quad \mathbf{v}_i + \tfrac{1}{2}\cot\left(\frac{\tilde{\psi}_i}{2}\right)\mathbf{R}(\mathbf{v}_{i-1} - \mathbf{v}_{i+1}) \end{aligned} \quad (9)$$

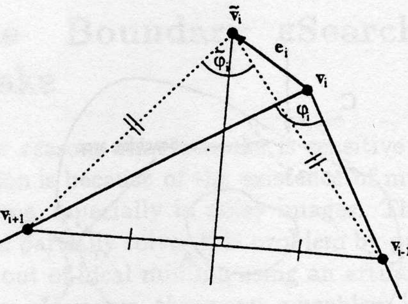

Figure 2: Local shape model.

where $\mathbf{R}$ is a $+90°$ rotation operation. Finally we come up with the second part of the internal energy formulation:

$$\mathbf{E}_{int(II)}(\mathbf{v}_i) = \frac{1}{2}\left(\frac{|\mathbf{e}_i|}{h}\right)^2 \quad (10)$$

and the complete internal energy is the sum of these two parts.

3.3 Improved Re-parameterization Procedure

The third modification is related to the re-parameterization procedure introduced in Ivins *et al.*'s paper. Since the snake starts with a small set of snaxels, more snaxels need to be added when the snake expands. Otherwise, the snaxels become too separated and miss important details. On the other hand, when a snake shrinks, surplus snaxels should be deleted to reduce processing requirements. In Ivins *et al.*'s implementation, the distance between any two adjacent snaxels is maintained between a pre-defined minimum and maximum. Whenever the distance between two snaxels is larger than the pre-defined maximum, one extra snaxel is added in the middle of the two snaxels. One of the snaxels is deleted when the distance is smaller than the given minimum. This poses as a problem since this procedure greatly reduces the stretch-resisting force from the internal energy formulation.

In our implementation, we add an extra snaxel to the middle of two snaxels when the following two conditions are met: (1) the distance between the two snaxels is larger than a pre-defined threshold; and (2) the difference between the angle, ψ (Fig. 2), and the average angle is less than a pre-defined threshold. The second condition is to prevent adding snaxels to rough places of the boundary where internal energy is building up. An example is shown in Fig. 3. In Fig. 3(A), an arrow is shown to indicate the place where internal energy is accumulating. One snaxel is trapped by a local minimum

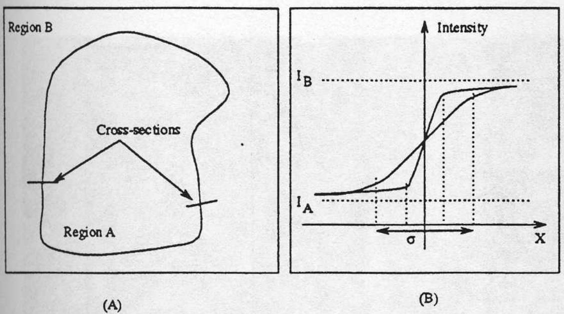

Figure 4: Generating testing images. (A) A hand-drawn irregular contour; and (B) edge profiles along the cross-sections.

(Fig. 3(B), (C), and (D)), and it is finally pulled out by its neighboring snaxels (Fig. 3(E)) when the accumulated internal energy is large enough. If extra snaxels were added to this place, this effect would be impossible to achieve (Fig. 3(F)).

4 Experimental Results

To evaluate the performance of the method we proposed we use both synthetic and real images, because using synthetic images provides us with a controllable testing environment, while real images can test the applicability of our method to practical problems.

To generate synthetic images, first an irregular closed contour is hand-drawn (Fig. 4(A)). The image generated based on this contour contains two regions, one inside the chosen shape and one outside. Thus the hand-drawn contour is the boundary separating these two regions. Each region is assigned an intensity value governed by a pre-defined contrast between these two regions. We further model the edge profiles along the boundary. In Fig. 4(A), some cross-section lines are shown; the intensity profiles for these lines, which are controlled by another parameter σ, are shown in Fig. 4(B). This way the synthesized images contain both sharp and gradual edges similar to those detected from ultrasound images. The parameter σ is randomly generated for some points on the boundary and interpolated for other points (Fig. 5(B)). Finally, Gaussian noise is added to the images; an example is shown in Fig. 5(D).

The boundary searching snake is applied to about 10 synthetic images[3] and results are promising. One example is shown in Fig. 6. Initialization (Fig. 6(B)) is easy since the boundary searching snake can successfully avoid being trapped in local minima. The result shown in Fig. 6(C) could be thought of that generated by an active region model based balloon. By comparing Fig. 6(C) and (G), it is clear that our model performs better at places with smooth boundary (indicated by an arrow in Fig. 6(C)). Results from other synthetic images show that our model has a consistent improvement over the balloon model.

[3] Only region information is used for synthetic images.

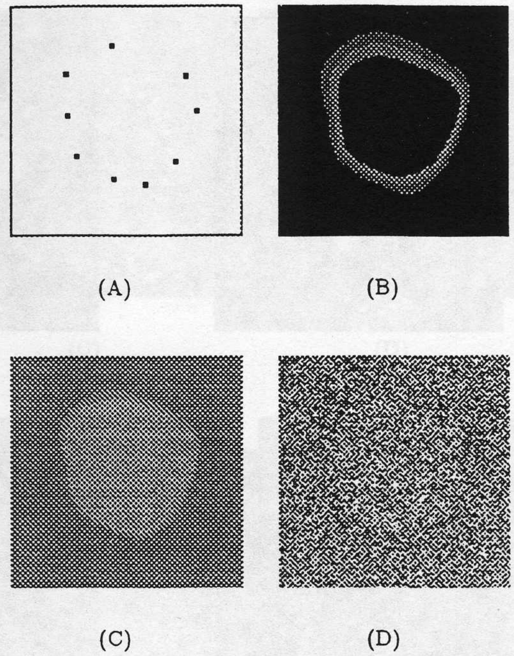

Figure 5: An example of generating testing images. (A) A hand-drawn contour; (B) transition areas; (C) the generated image (intensities of the inner and outer part are 170 and 150 respectively); (D) the image with Gaussian noise (with a standard deviation of 50) added.

Our model is also applied to several ultrasound images of pork loins. One example is shown in Fig.7. We used an edge aggregation method based on Sha'ashua and Ullman's *saliency map* method [7] to generate an edge map (Fig. 7(D)). Details will be reported in a later paper. The edge map is used as the potential field for the boundary searching snake. Fig. 7(B) shows the first equilibrium state and the corresponding saliency map with the snake superimposed is shown in Fig. 7(E). Note that in Fig. 7(E), a circle is shown to highlight a piece of weak edge which has been skipped. The final result, which is the fifth equilibrium state, is shown in Fig. 7(C). Dotted lines in Fig. 7(F) show the correct boundary drawn by an expert for the bottom-right part.

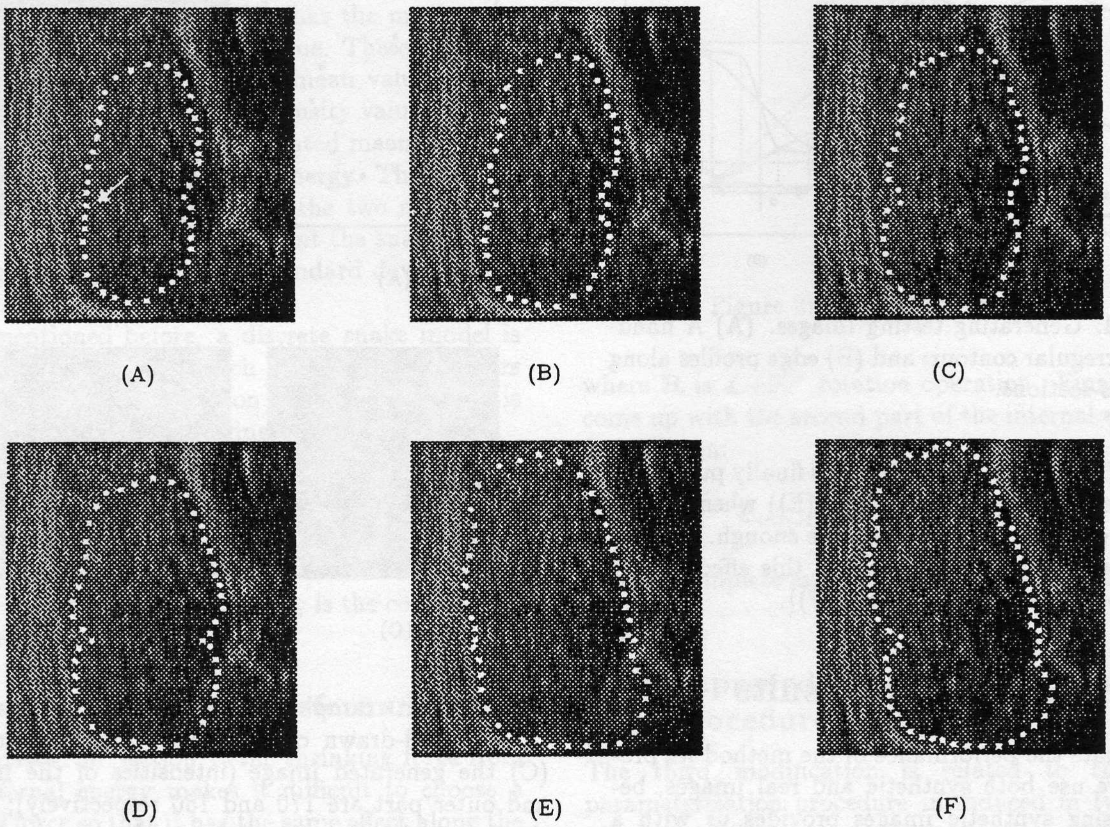

Figure 3: An illustration of the improved re-parameterization procedure. (A) A snake which is put on an image of pork loins. The arrow indicates the place where internal energy is building up. (B)-(D) The internal energy is getting larger and no snaxels have been added to this area. (E) The snaxel which was trapped in the local minimum has been successfully pulled out. (F) The result produced by a snake with the original re-parameterization procedure.

By comparing Fig. 7 (B) and (C), we can easily observe that the boundary searching snake can more effectively use weak information.

5 Conclusion

Minimization of snake energy has been plagued by the existence of multiple local minima in noisy images. In this paper we have demonstrated a snake searching strategy that alleviates this problem to a large extent. The searching strategy is achieved by systematically changing the direction and magnitude of an artificial normal force. The added force is initially chosen to be large and outgoing, but is later flipped in direction and reduced in magnitude after reaching equilibrium. The process is then repeated until the normal force is small compared to the other snake forces. The proposed technique thus effectively performs a multi-level feature search that uses both strong and weak image information. Moreover, our snake model becomes less sensitive to its initialization since it is not trapped in local minima as easily as other existing snake models. The searching area is also restricted by results obtained during previous iterations and thus the extra computation required is not significant. We have presented some promising results from an implementation based on an active region model. In addition, the efficacy of a number of improvements to this model have been demonstrated: (1) both edge and region information are used to minimize the uncertainty in segmentation; (2) an adaptive feature is added to cope with images with slowly changing background intensity; (3) the internal energy is reformulated to get rid of the original shrinking tendency; and (4) the re-parameterization procedure is improved so that the internal stretch-resisting force is not impaired.

This paper reports the first step we have done in segmenting noisy images. Currently we are inves-

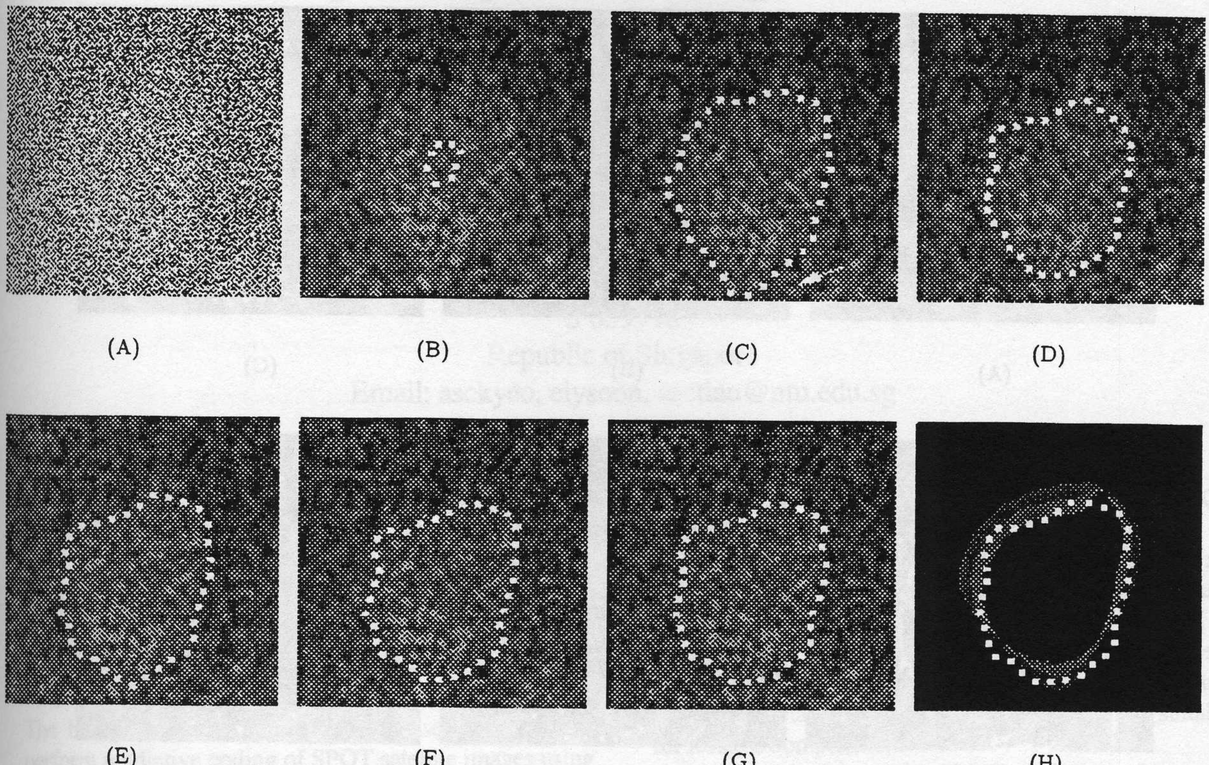

Figure 6: An example of the boundary searching snake. (A) The image to be processed. (B) Initialization of the contour. The image is smoothed by a Gaussian filter and its intensity is transformed by a histogram equalization algorithm. (C) The first equilibrium. This time the normal force is chosen to be large and outgoing. (D)-(G) The next four equilibrium states. Each time the direction of the normal force is flipped and the magnitude reduced to 80%. (H) The seed contour with the recovered contour superimposed.

tigating image smoothing and edge detecting techniques for noisy images. The purpose of this step is to provide a boundary searching snake with a set of reliable edges. We also try to analyze the data collected by a snaxel when it travels during the searching. Future work also includes applying our method to segmentation of texture images.

References

[1] M.-O. Berger and R. Mohr. Towards autonomy in active contour models. In *Proceedings of Int'l Conference on Pattern Recognition*, pages 847–851. IEEE Press, 1990.

[2] L. D. Cohen and I. Cohen. Finite-element methods for active contour models and balloons for 2-D and 3-D images. *IEEE Transactions on Pattern Analysis and Machine Intelligence*, 15(11):1131–1147, 1993.

[3] S. R. Gunn and M. S. Nixon. A robust snake implementations: A dual active contour. *IEEE Transactions on Pattern Analysis and Machine Intelligence*, 19(1):63–68, 1997.

[4] J. Ivins and J. Porrill. Active region models for segmenting textures and colours. *Image and Vision Computing*, 13(5):1995, 431–438.

[5] M. Kass, A. Witkin, and D. Terzopoulos. Snakes: Active contour models. *Int'l Journal of Computer Vision*, 1(4):321–331, 1988.

[6] F. Leymarie and M. D. Levine. Tracking deformable objects in the plane using an active contour model. *IEEE Transactions on Pattern Analysis and Machine Intelligence*, 15(6):617–643, 1993.

[7] A. Shaashua and S. Ullman. Structural saliency: The detection of globally salient structures using a locally connected network.

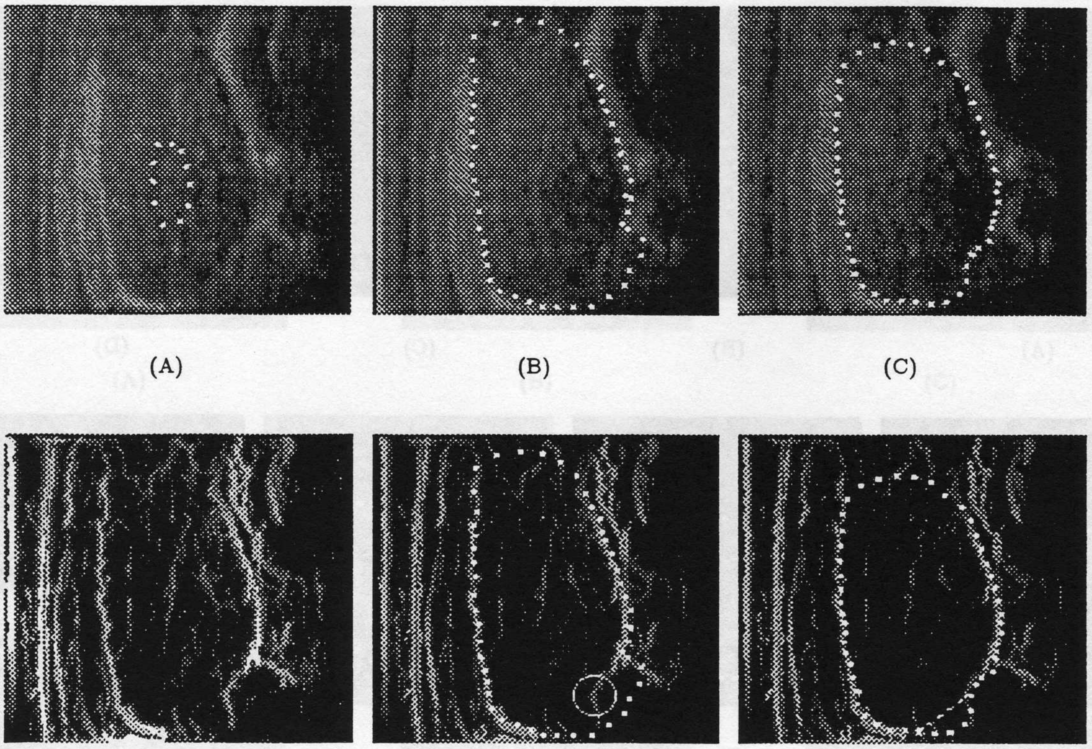

(A) (B) (C)

(D) (E) (F)

Figure 7: An example of the boundary searching snake applied to an ultrasound image. (A) A boundary searching snake initialized on an ultrasound image; (B) the first equilibrium; (C) the final result; (D) the corresponding edge map; (E) the edge map superimposed with the result from the first equilibrium (A circle is drawn to highlight a piece of weak edge which has been skipped); (F) the edge map superimposed with the final result (Dotted lines indicate the correct boundary position given by an expert).

In *Proceedings of Int'l Conference on Computer Vision*, pages 321–327. IEEE Press, 1988.

[8] A. A. Aminiand T. E. Weymouth and R. C. Jain. Using dynamic programming for solving variational problems in vision. *IEEE Transactions on Pattern Analysis and Machine Intelligence*, 12(9):855–867, 1990.

[9] D. J. Williams and M. Shah. A fast algorithm for active contours. In *Proceedings of Int'l Conference on Computer Vision*, pages 592–595. IEEE Press, 1990.

[10] G. Xu, E. Segawa, and S. Tsuji. Robust active contours with insensitive parameters. *Pattern Recognition*, 27(7):879–884, 1994.